International Journal of Emerging Engineering and Technology (IJEET)
ISSN (e): 2958-3764
Volume: 3, Number: 1, Pages: 9 - 16, Year: 2024

# Optimizing the Corrosion Protection Performance Of Epoxy Coatings for Cu Substrates: An Electrochemical Perspective

Usman Khan[1], Nouman Khan[2], Arshad Ali Khan[3*], Ishaq Ahmad[1], Zainab Zafar[1]

[1] National Centre for Physics, Quaid-i-Azam University Campus, Postcode 45320, Islamabad, Pakistan

[2] Faculty of Engineering Sciences, Ghulam Ishaq Khan Institute of Engineering Sciences and Technology, Topi, 23640, KPK, Pakistan

[3] Department of Mechanical Engineering, University of Engineering and Technology, Postcode 25120, Peshawar, Pakistan

[*]Corresponding Author: Arshad Ali Khan (Email Address: engrarshad@uetpeshawar.edu.pk)

***Abstract*— Saline water triggers the inevitable progression of corrosion risk in marine equipment, driven by spontaneous electrochemical reactions. This study used dip coating technique to prepare copper (Cu) substrates coated with epoxy resin. The study aimed to determine the optimal coating curing temperature and the epoxy-hardener ratio to exhibit maximum corrosion resistance for the epoxy-coated Cu. A comprehensive analysis of the curing temperature within the designated 40 to 120°C range and molarity of 0.6M-1.8M was conducted. The corrosion response of Cu substrates was evaluated using the electrochemical measurements of linear polarization resistance (LPR), potentiodynamic curve, and electrochemical impedance spectroscopy (EIS). The study reveals that the corrosion resistance (Rc) notably increases until reaching its peak at the optimal temperature value of 90°C and epoxy-hardener ratio of 2:1. Furthermore, a correlation between corrosion rate and molarity increased results in the deterioration of the coated surface.**

***Keywords*— Corrosion, epoxy resin, electrochemical reactions, curing temperature, electrochemical impedance spectroscopy***

## I. INTRODUCTION

Cu is a versatile metal with widespread uses across diverse industrial sectors. It is prominently employed in various industrial applications such as electrical power lines, pipelines, heat exchangers, and numerous other industrial uses [1, 2]. The extensive array of applications for Cu stems from its exceptional electrical, mechanical, and thermal properties, combined with its notable resistance to corrosion [3]. On the other hand, aggressive mediums such as sulphide [4], ammonia ions [5], and chloride [6] can cause it to corrode. Cu has a considerable potential for corrosion in saltwater, mostly due to the presence of chloride ions and oxidized oxygen, which accelerate the corrosion process [6-10]. Chloride ions primarily cause the corrosion of marine Cu equipment, while other elements also play a part, such as salinity [11], pH [12], and seawater flow [13, 14]. Epoxy resins (ERs) are well-known polymeric materials with a wide range of applications such as electronic encapsulation, for laminates, adhesives, and anti-corrosive coatings [15-18] curatives, resulting in the formation of cross-linked macromolecular molecules. These involve aliphatic and aromatic alcohols, thiols [19, 20], and polyfunctional aliphatic and aromatic amines, including acid derivatives (such as acid chlorides, amides, esters, and anhydrides).

The cross-linking curing reactions yield thermosetting polymers with superior mechanical strength and outstanding thermal and chemical stability [21]. ERs display many captivating properties, encompassing a broad spectrum of varieties that can be achieved by manipulating and modifying the hardener or curing agent composition [22]. These variations enable the production of ERs from low-viscosity liquids to high melting point solids. Since ERs naturally undergo curing at various temperatures, it is possible to modify essential features, including mechanical strength, thermal stability, chemical resistance, and flexibility. Because of its adaptability, ERs may be tailored to meet specific demands and requirements for various applications [23].

In recent times, ERs have gained significant popularity as highly effective anti-corrosive coatings. Polymeric epoxies adhere at the interface between the corroded environment and metallic surfaces to create physical barriers, reducing the corrosion rate [24]. The widespread usage of epoxy resin coatings can be attributed to their remarkable thermal and chemical stabilities and exceptional mechanical strength [25]. Moreover, most ERs demonstrate robust adhesion capabilities to metallic surfaces, owing to their high surface or peripheral functionalities that facilitate excellent interactions through a donor-acceptor mechanism [15, 26-28]. However, two factors significantly contribute to the corrosive resistant potential of epoxy coating: one is the curing temperature at which the epoxy-coated substrate undergoes curing [29, 30], and the other is the epoxy-to-hardener composition ratio, which ensures the formation of a dense and impermeable barrier when the epoxy cures [31-33]. In addition, Cu corrosion in seawater is also influenced by dissolved salt ions, which cause the electrochemical corrosion to increase through electrolytic conductivity. Moreover, the molarity or concentration of seawater greatly

affects the corrosion process, as higher seawater salinity enhances the rate of Cu corrosion [34] .

This study employs a controlled experiment approach in which Cu substrates were subjected to different epoxy coatings having different epoxy-to-hardener ratios, i.e., 1:1, 1.5:1, 2:1 & 2.5:1. The aim was to find the optimum value of the epoxy to hardener ratio which gives the maximum corrosion resistant potential keeping the curing temperature and seawater molarity constant. Also, the impact of curing temperature at a fixed epoxy-to-hardener ratio and seawater molarity was investigated. Lastly, the corrosion effect of synthetic seawater on epoxy-coated Cu substrate was studied with constant optimum values of epoxy-to-hardener ratio and curing temperature.

## II. MATERIALS AND METHODS

### *A. Sample Preparation*

Cu substrates were made by precisely cutting Cu sheets into square samples that were 20 * 10 * 5 mm thick. Before the coating process, the substrates underwent mechanical polishing using SiC paper with grit sizes ranging from 80 to 2000, then rinsing with distilled water. In continuation, the substrates were subjected to sonication in acetone to eliminate any residual grease, after which they were meticulously washed with distilled water. Subsequently, the substrates were air-dried at room temperature.

### *B. Preparation of Epoxy Mixture*

The milky emulsion of the polymeric epoxy resin (Waterpoxy 1422) and the amine hardener (Waterpoxy 751) were procured from BASF, a chemical company headquartered in Germany. To serve as a coating, epoxy resin and hardener mixtures were prepared at different epoxy resin-to-hardener mass ratios of 1:1, 1.5:1, and 2:1. Furthermore, mechanical mixing was employed to achieve a homogeneous blend, ensuring uniformity in the resulting mixtures. The complete methodology for sample preparation is depicted in **Fig.1**.

### *C. Coating of Epoxy on Cu substrates*

Following the preparation of the epoxy mixture, the Cu metal samples were subjected to dip coating. Subsequently, the coated samples underwent curing at different temperatures, ranging from 40°C to 120°C with a temperature increment of 10°C. The thickness of the coating on the substrate was110±5µm. After determining the optimized temperature and epoxy resin-to-hardener ratio, samples were prepared and exposed to synthetic seawater solutions with varying molarities, i.e., 0.6M, 1.2M, and 1.8M.

### *D. Electrochemical characterization*

The linear Polarization Resistance (LPR), electrochemical impedance spectroscopy (EIS), and potentiodynamic (PD) measurements were conducted using the Gamry Potentiostat System. The Nyquist plots were collected for all the data during the EIS testing while preserving the frequency range of 100,000 to 0.1 Hz. Pot potentiodynamic curves were produced in the (-0.1-1V) electrical potential range for all the samples.

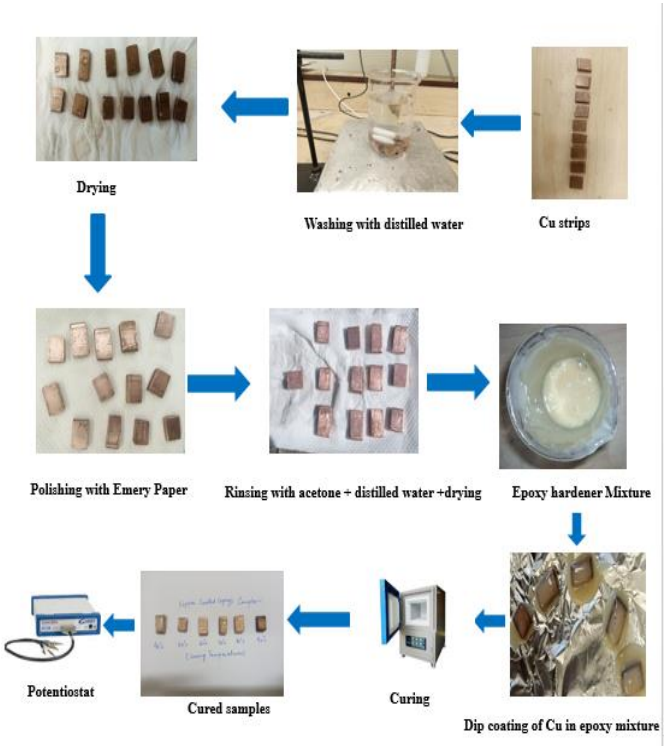


Fig.1 Complete methodology and activities performed for the research work

## III. RESULTS AND DISCUSSION

### *A. Linear Polarization Resistance Analysis of epoxy-Cu at different curing Temperatures*

Linear Polarization Resistance (LPR) analysis assessed the corrosion resistance behaviour of epoxy-coated Cu samples. In the initial phase, samples were cured at various temperatures, and a three-electrode potential setup was employed using the Gamry framework. The results indicated that at lower curing temperatures (40°C and 60°C), the epoxy coatings exhibited inadequate adhesion to the metal surface, leading to fluctuating resistance values, as justified by Fig. 2.

A more stable behaviour was observed as the curing temperature increased, resulting in promising results at 70°C with a resistance value of 13.59 kΩ and an equivalent CR of 0.8757 may. Surprisingly, the highest corrosion resistance was achieved at 90°C, surpassing the value obtained for the 70°C cured composite by a significant factor of 4.86. Beyond this point, a decline in corrosion resistance was evident when curing temperatures were raised to 100°C, 110°C, and

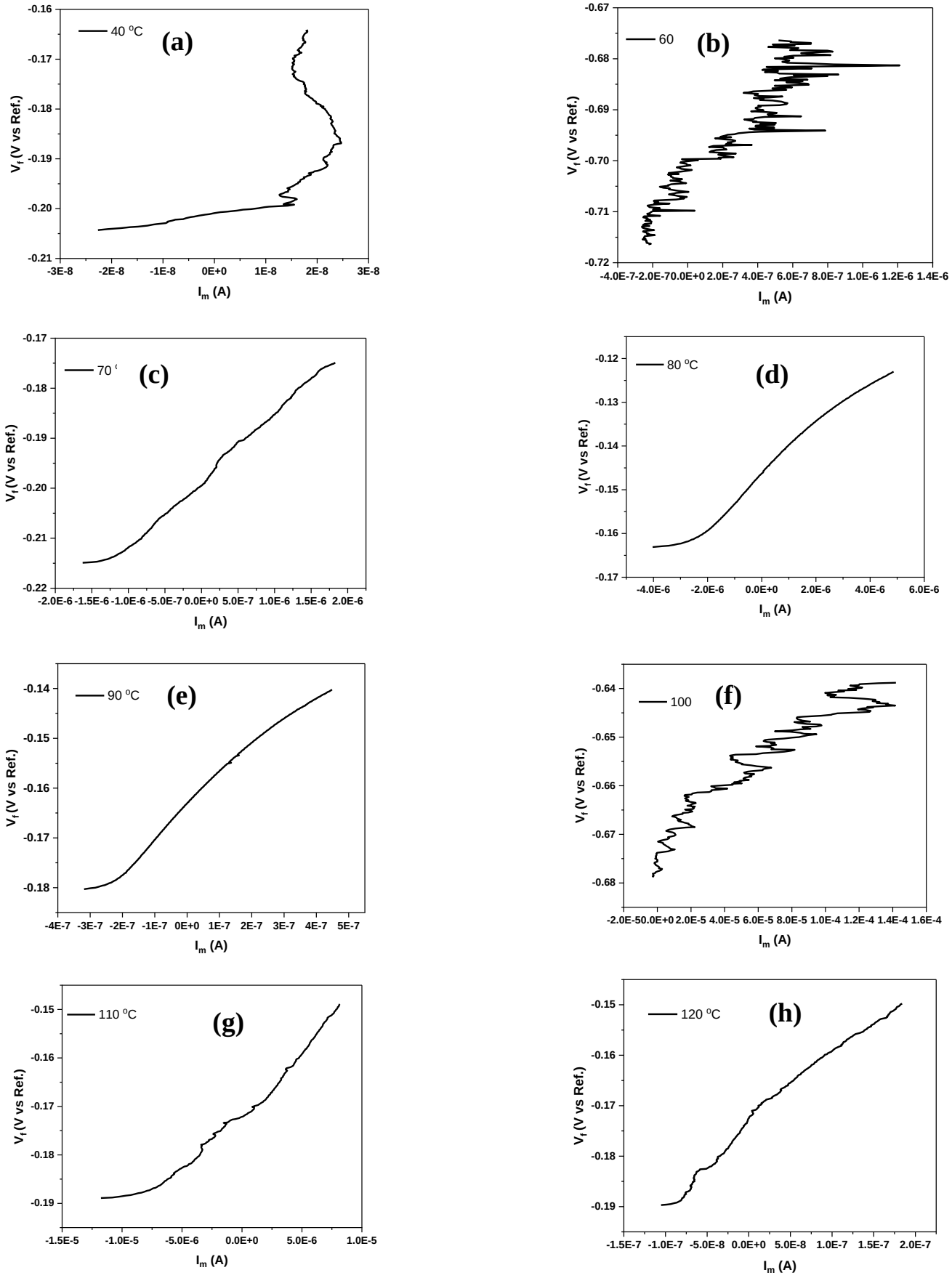


Fig.2 Linear polarization resistance plots of Cu coated with epoxy at different curing temperatures (for fixed 0.6M solution & epoxy-hardener ratio 2:1)

120°C, reaffirming that 90°C is the optimal curing temperature as depicted in Fig. 2 and Table 1. The findings of this investigation indicate that the corrosion resistance of the Cu composite is greatly influenced by controlling the curing temperature during the epoxy coating process.

TABLE 1 LPR AND CR OF CU COATED WITH EPOXY AT DIFFERENT CURING TEMPERATURES

| Temperature (°C) | LPR (kΩ) | CR (mpy) |
|---|---|---|
| 70 | 13.59 | 0.8757 |
| 80 | 26.14 | 0.4323 |
| 90 | 66.05 | 0.1802 |
| 100 | 39.41 | 0.312 |
| 110 | 20.562 | 0.579 |
| 120 | 4.275 | 1.17 |

### *B. Linear Polarization Resistance Analysis of epoxy-Cu at varying Epoxy to Hardener Ratio*

Fig.3 and Table 2 demonstrate the impact of varying epoxy resin-hardener ratios on the corrosion resistance of the copper coating. A CR of 0.1802 mpy and a corrosion resistance of 66.05 kΩ were achieved with an optimal ratio of 2:1.Deviating from this ratio resulted in incomplete polymerization showed inadequate curing at lower ratios and incomplete curing at higher ratios. Controlling the epoxy-to-hardener ratio ensures efficient and durable corrosion protection for copper components.

TABLE 2 LPR AND CR OF EPOXY-CU WITH VARYING EPOXY-HARDENER RATIO

| Epoxy-hardener Ratio | LPR (kΩ) | CR (mpy) |
|---|---|---|
| **1:1** | **51.8** | **0.2298** |
| **1.5:1** | **62.36** | **0.1909** |
| **2:1** | **66.05** | **0.180** |
| **2.5:1** | **59.61** | **0.214** |

### *C. Linear Polarization Resistance Analysis of epoxy-Cu at varying Molarities*

Additionally, Fig.4 and table 3 illustrate the Linear Polarization Resistance (LPR) response concerning the molarity of a synthesized sample, prepared at the optimal curing temperature (90°C) and with an epoxy-hardener ratio of 2:1. Notably, the corrosion resistance exhibited an inverse relationship with the molarity of the artificially prepared seawater solution. Specifically, at 0.6M solution, the corrosion resistance was 37.03 and 10.24 times lower than the resistance observed for the samples immersed in 1.8M and 1.2M solutions, respectively.

This observed behavior can be attributed to the presence of ions, such as Na and Cl, which play a essential role in the electrochemical reactions occurring at the surface. Higher molarity corresponds to an increased number of ions, resulting in a higher CR and reduced corrosion resistance.

TABLE 3 LPR AND CR OF EPOXY-COATED CU IN DIFFERENT SEAWATER MOLARITY

| Molarity (M) | LPR (kΩ) | CR (mpy) |
|---|---|---|
| **0.6** | **63.25** | **0.17** |
| **1.2** | **17.5** | **0.05** |
| **1.8** | **1.708** | **6.97** |

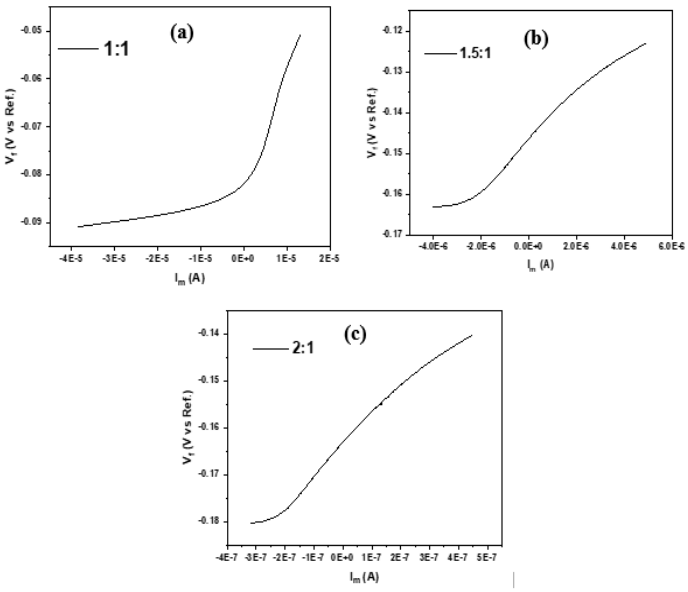


Fig.3 Effect of varying epoxy resin and hardener ratio on LPR as a coating mixture on Cu (at fixed curing temperature=$90^0$C & molarity=0.6M)

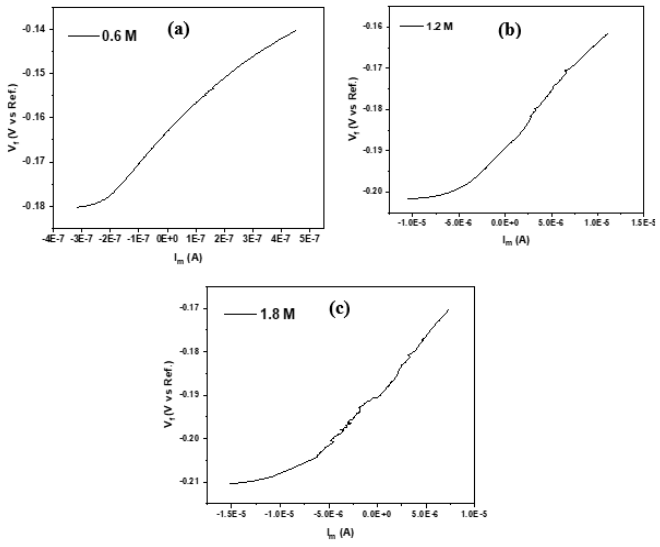


Fig.4 LPR Behavior of epoxy-coated Cu in different molarities of synthetic seawater solution

### D. *Linear Polarization Resistance Analysis of Bare-Cu in different Seawater molarities*

It is evident from Fig.5 that the resistance of uncoated copper against corrosion also declines when exposed to harsher seawater conditions. The increase in seawater molarity leads to higher Na and Cl ion concentrations, decreasing LPR. Fig. 5 presents the LPR values of bare copper at molarities of 0.6M, 1.2M, and 1.8M, with constant curing temperature and epoxy-hardener ratio. The LPR values for bare copper are 1.708 kΩ at 1.8M, 0.5707 kΩ at 1.2M, and the lowest value of 0.0018 kΩ at 0.6M. Corresponding CRs are 32.4 mpy, 20.86 mpy, and 6.971 mpy, respectively, as demonstrated in Table 4. This data demonstrates the detrimental effect of increasing seawater molarity on bare copper corrosion resistance. The findings emphasize the importance of protective coatings and corrosion mitigation strategies to safeguard copper materials from corrosion in varying seawater environments.

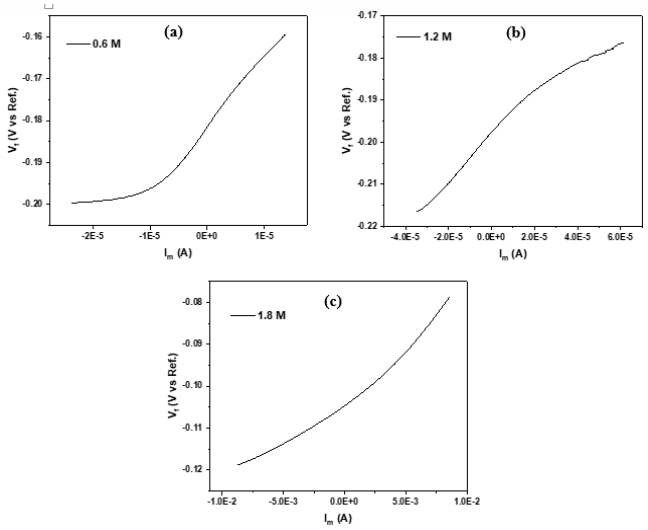


Fig.5 LPR Behavior of bare Cu in different molarities of synthetic seawater solution (fixed curing temperature and epoxy-hardener ratio=2:1)

TABLE 4 LPR AND CR OF BARE CU IN DIFFERENT SEAWATER MOLARITY

| Molarity (M) | LPR (kΩ) | CR (mpy) |
|---|---|---|
| 0.6 | 1.708 | 6.971 |
| 1.2 | 0.5707 | 20.86 |
| 1.8 | 0.001842 | 32.4 |

### E. *EIS Investigations*

The Nyquist plot constitutes a graphical technique extensively applied in the scrutiny of electrochemical systems impedance behaviors. Fig. 6(a) is a graphical representation that portrays epoxy-coated copper samples subjected to distinct curing temperatures of 80°C, 90°C, and 120°C. The dimension of the semicircular arc in the plot is indicative of the corrosion resistance exhibited by each specimen. Specifically, greater semicircle diameters correlate with higher corrosion resistance. A larger semicircle diameter corresponds to a higher charge transfer resistance. Notably, the graphical illustration underscores that the polymer-coated metal, when cured at 90°C, manifests the most pronounced resistance to corrosion, surpassing its counterparts cured at 80°C and 120°C in this regard. Similarly, in Fig. 6(b) and 6(c), the Nyquist plots reveal that the most substantial semicircle diameter was achieved for the composite coated with an epoxy-hardener ratio of 2:1 and a concentration of 0.6M, signifying the optimal formulation of epoxy and hardener components. Additionally, an observed trend indicated that an escalation in solution molarity led to reduced corrosion resistance.

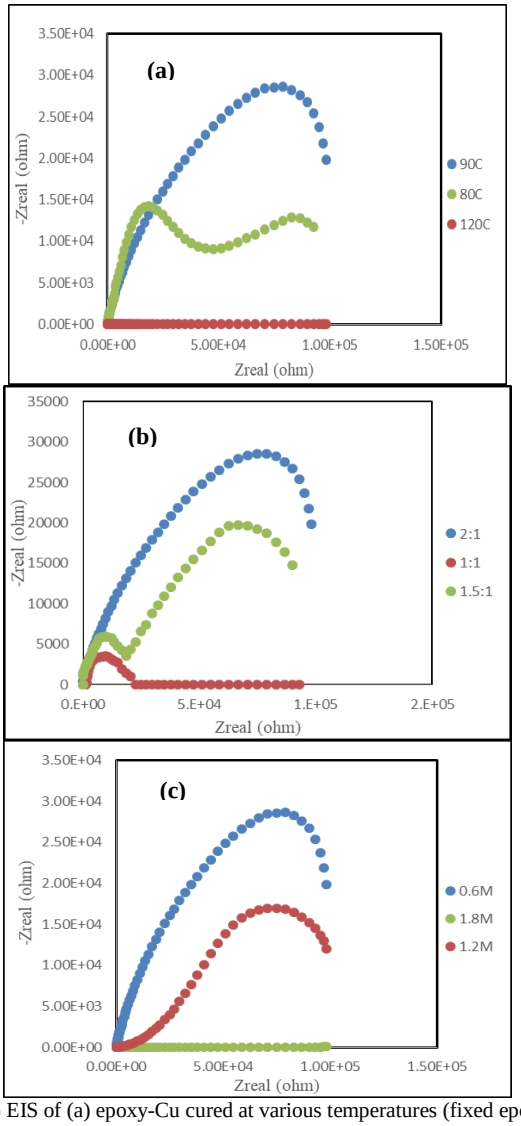


Fig.6 EIS of (a) epoxy-Cu cured at various temperatures (fixed epoxy-hardener ratio=2:1 & molarity=0.6M) (b) prepared in various epoxy-hardener ratio (fixed curing temperature=90$^0$C & molarity=0.6M) (c) experimented in varying molarities of synthetic seawater (fixed epoxy-hardener ratio=2:1 & curing temperature=90$^0$C)

Fig.7 shows the effect of the curing temperature of the epoxy-Cu on the linear LPR and the CR. The graphical representation illustrates a notable inverse correlation between the LPR and the CR. Initially, the trend elucidates that elevating the curing temperature of the Cu-epoxy composite results in an augmentation of LPR, which attains its zenith at 90°C at which the LPR is 66.05 KΩ and the corresponding CR is 0.1802 mpy. Nonetheless, a subsequent

temperature rise beyond 90°C exhibits a concomitant escalation in CR, coinciding with a reduction in LPR. This observed phenomenon can be attributed to the interplay of competing factors. The rise in LPR up to 90°C indicates improved corrosion resistance, as increased curing temperature promotes enhanced cross-linking and polymer network formation within the composite, leading to a more protective surface. The subsequent decline in LPR beyond 90°C might be attributed to the potential degradation of the epoxy due to prolonged exposure to higher temperatures, inducing a compromise in its corrosion resistance.

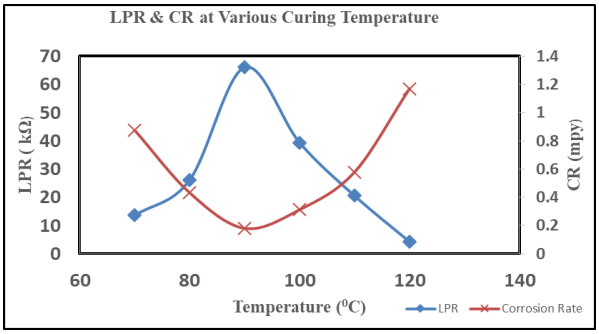


Fig.7 Trend of LPR and CR at various curing temperatures

The graph effectively demonstrates the epoxy-hardener ratio's pivotal role in shaping the LPR and CR of the material under investigation. The discernible trend in Fig.8 underscores that an optimal ratio of 2:1 for the epoxy resin and hardener mixture yields the most favourable outcome, signifying a paramount influence on corrosion inhibition. However, an increase in the epoxy ratio adversely influences the corrosion inhibition response of the specimen. This observed trend can be attributed to the intricate interplay between the epoxy-hardener composition and the material's corrosion resistance properties. The ideal epoxy-hardener ratio of 2:1 likely corresponds to a balanced ratio that optimally promotes cross-linking and polymer network formation within the material's matrix. This results in an enhanced protective surface, effectively hindering the onset of corrosion. On the contrary, an excessive epoxy ratio beyond this optimal point might introduce an imbalance in the cross-linking structure, potentially leading to compromised protective layers or decreased adhesion properties.

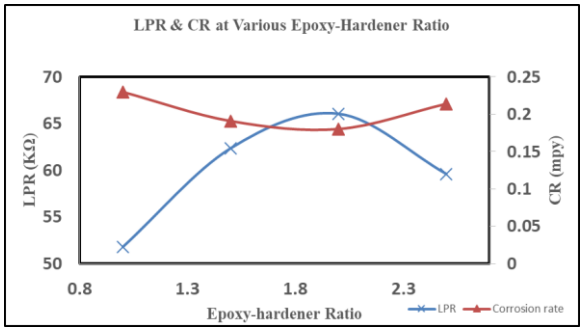


Fig.8 Behavior of LPR and CR at varying epoxy-hardener ratio

Fig. 9 (a) and Fig. 9(b) elucidate the impact of varying molar concentrations of synthetic seawater on the LPR and CR of Cu epoxy-hardener (2:1) coated and bare Cu samples, respectively. Notably, the figure reveals a downward trajectory in LPR as the molarity of the NaCl solution escalates. This observation indicates an augmented susceptibility of the coated Cu epoxy-hardener (2:1) and bare Cu specimen to corrosion within more concentrated NaCl solutions. This trend is reasonably attributed to the intricate electrochemical mechanisms at play. Higher molarities of NaCl solution contribute to an elevated concentration of chloride ions at the sample's surface. These chloride ions play a pivotal role in initiating localized corrosion processes, such as pitting corrosion, by accelerating the creation of localized anodic regions on the material's surface. This phenomenon ultimately leads to a reduction in LPR, which reflects compromised corrosion resistance.

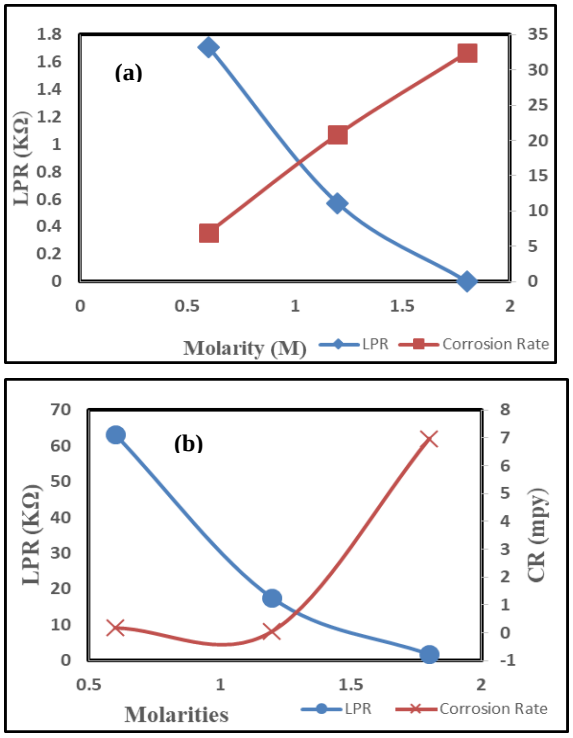


Fig.9 In varying synthetic seawater molarities (a) LPR and CR response of Cu-epoxy sample (b) LPR and CR behavior of bare Cu

## *F. Potentiodynamic polarization*

Figure 10 represents the current response of epoxy-coated Cu samples cured at different temperatures when the potential is linearly scanned from a cathodic to an anodic direction. This technique is called potentiodynamic linear scan voltammetry. The current response depends on the electrochemical reactions at the electrode surface and the kinetics of these reactions.

The electrochemical behaviour of three different epoxy-coated samples, cured at 90°C, 80°C, and 120°C, was investigated through potentiodynamic curves. An increase in potential for the sample cured at 90°C led to a corresponding rise in cathodic current, reaching a maximum at the passivation potential (Epp). At this point, a thin epoxy film formed on the metal surface, reducing the CR. Subsequently, the current decreased in the passivity region where the stable and protective oxide film was established. No breakdown phenomena were observed in the blue curve, implying the epoxy coating's resistance to pitting and dissolution.

Conversely, the potential increase for the sample cured at 80°C decreased the cathodic current, reaching a minimum at the corrosion potential (Ecorr) where anodic and cathodic currents equalled. Beyond this point, the current rapidly

increased in the anodic region, indicating predominant metal dissolution. The absence of passivation or breakdown phenomena in the red curve indicated the lack of protective oxide film or coating.

Notably, the 120°C-cured specimen exhibited the lowest corrosion resistance. This was evident from its high current values in both cathodic and anodic regions, reflecting elevated rates of electrochemical reactions and metal dissolution. The absence of distinct passivation behaviour and the lack of clear maximum or minimum current in the red curve indicated corrosion in an acidic environment where metal dissolution dominated.

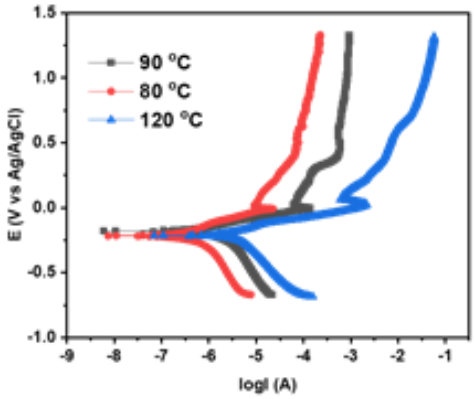


Fig.10 Tafel's plot of epoxy-coated Cu cured at varying temperatures.

The graph in Fig.11 illustrates the CR observed in epoxy-coated copper samples of varying molarity immersed in artificial seawater solutions. The discernible trend in the graph showcases a direct relationship: as the molarity of the seawater increases, so does the CR of the copper samples. This observed correlation can be attributed to the elevated presence of corrosive agents, such as chloride ions, within the higher molarity seawater solutions.

The underlying mechanism driving this behaviour resides in the intensified concentration of aggressive elements within the seawater. These corrosive agents can breach the protective epoxy coating and access the underlying copper substrate. While the epoxy coating is fundamentally designed to establish a barrier between the metal and the surrounding environment, it might not exhibit adequate resistance to the seawater's heightened salinity and aggressive nature at elevated molarities.

Under such conditions, the epoxy coating could undergo structural deterioration, such as cracking, peeling, or blistering. These alterations could allow electrochemical reactions to transpire, compromising the integrity of the protective barrier. Consequently, the copper substrate becomes exposed to the corrosive influences of the seawater environment. It follows that an augmentation in seawater molarity exacerbates the severity of these detrimental effects, leading to an escalation in the CR of the epoxy-coated copper samples.

The tripartite curves depicted in Fig.11 correspond to the potentiodynamic scans of a metallic substrate, illustrating its susceptibility to corrosion within a synthetic seawater environment. A direct correlation between the curve's gradient and CR is evident, with higher slopes indicative of accelerated CR. Consequently, the red curve, displaying the steepest slope, signifies the highest CR apart from the blue and purple counterparts.

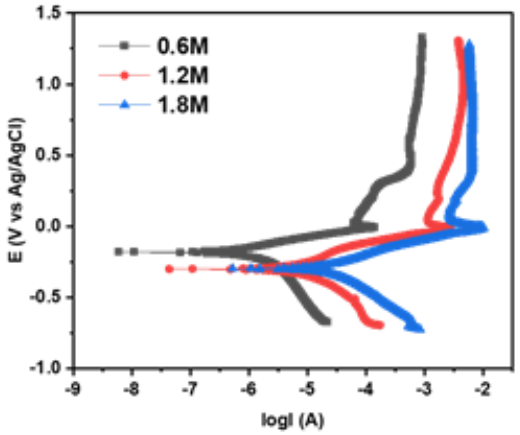


Fig.11 Tafel's plot: highlighting the effect of molarity of synthetic seawater on prepared coated samples.

Within this context, the specimen featuring an epoxy-hardener ratio of 1.5:1 attains a CR lower than that delineated by the purple curve but surpasses the CR observed along the red trajectory. Conversely, the copper substrate coated with epoxy-hardener in a 2:1 ratio registers the most subdued CR across the entire ensemble of curves, as shown in Fig.12. Thus, optimal corrosion resistance is associated with reduced curve gradients, advocating for minimized slope steepness.

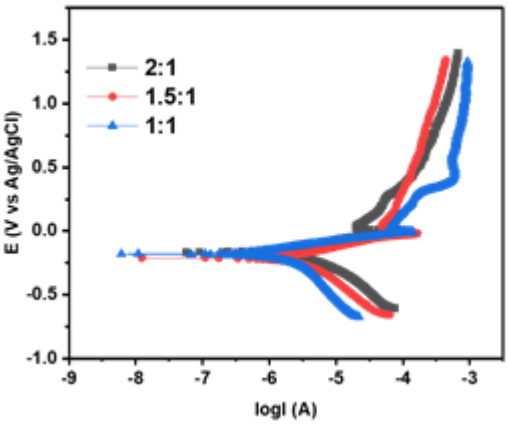


Fig. 12: Effect of different epoxy-hardener compositions depicted by Tafel's plot.

## IV. CONCLUSIONS

- A comprehensive investigation was conducted on the curing temperature within the designated range of 40 to 120°C, with a temperature difference of 10°C, along with the epoxy-to-hardener ratios set at 1:1, 1.5:1, 2:1, and 2.5:1.
- The coating with the epoxy-hardener ratio of 2:1 on Cu substrates showed significant corrosion resistance at intermediate temperatures and lower molarity of the electrolytic solution.
- The study uncovers a significant connection: as the curing temperature rises, the composite's corrosion resistance (Rc) notably increases until reaching its peak at the optimal temperature value of 90°C and epoxy-hardener ratio 2:1.
- Moreover, this research work revealed a strong association wherein the corrosion rate exhibited a

proportional escalation with the increasing molarity of the synthetic seawater solution, consequently resulting in the degradation of the coated surface.

## ACKNOWLEDGMENT

The authors greatly appreciate the technical support of the National Centre for Physics Islamabad, Pakistan.

## REFERENCES

[1] Amin, M.A. and K. Khaled, Copper corrosion inhibition in O2-saturated H2SO4 solutions. Corrosion Science, 2010. 52(4): p. 1194-1204.

[2] Dahmani, K., et al., Quantum chemical and molecular dynamic simulation studies for the identification of the extracted cinnamon essential oil constituent responsible for copper corrosion inhibition in acidified 3.0 wt% NaCl medium. Inorganic Chemistry Communications, 2021. 124: p. 108409.

[3] Sherif, E.-S.M., R. Erasmus, and J. Comins, Corrosion of copper in aerated synthetic sea water solutions and its inhibition by 3-amino-1, 2, 4-triazole. Journal of colloid and interface science, 2007. 309(2): p. 470-477.

[4] Šekularac, G. and I. Milošev, Corrosion of aluminium alloy AlSi7Mg0. 3 in artificial sea water with added sodium sulphide. Corrosion Science, 2018. 144: p. 54-73.

[5] Davalos-Monteiro, R., Observations of corrosion product formation and stress corrosion cracking on brass samples exposed to ammonia environments. Materials Research, 2018. 22: p. e20180077.

[6] Otmačić, H., et al., Protective properties of an inhibitor layer formed on copper in neutral chloride solution. Journal of Applied Electrochemistry, 2004. 34: p. 545-550.

[7] Sherif, E. and S.-M. Park, Inhibition of copper corrosion in 3.0% NaCl solution by N-phenyl-1, 4-phenylenediamine. Journal of the Electrochemical Society, 2005. 152(10): p. B428.

[8] Pan, Y.-C., et al., 2-Amino-5-(4-pyridinyl)-1, 3, 4-thiadiazole monolayers on copper surface: Observation of the relationship between its corrosion inhibition and adsorption structure. Corrosion science, 2013. 73: p. 274-280.

[9] Sherif, E. and S.-M. Park, 2-Amino-5-ethyl-1, 3, 4-thiadiazole as a corrosion inhibitor for copper in 3.0% NaCl solutions. Corrosion science, 2006. 48(12): p. 4065-4079.

[10] Curkovic, H.O., E. Stupnisek-Lisac, and H. Takenouti, The influence of pH value on the efficiency of imidazole based corrosion inhibitors of copper. Corrosion Science, 2010. 52(2): p. 398-405.

[11] Wang, B., et al., Atmospheric corrosion of aluminium alloy 2024-T3 exposed to salt lake environment in Western China. Corrosion Science, 2012. 59: p. 63-70.

[12] Lytle, D.A. and M.R. Schock, Pitting corrosion of copper in waters with high pH and low alkalinity. Journal - American Water Works Association, 2008. 100(3): p. 115-129.

[13] Xia, J., et al., Effect of Flow Rates on erosion corrosion behavior of hull steel in real seawater. International Journal of Electrochemical Science, 2021. 16(5): p. 210532.

[14] Wood, R., S. Hutton, and D. Schiffrin, Mass transfer effects of non-cavitating seawater on the corrosion of Cu and 70Cu-30Ni. Corrosion Science, 1990. 30(12): p. 1177-1201.

[15] Hsissou, R., et al., Rheological properties of composite polymers and hybrid nanocomposites. Heliyon, 2020. 6(6).

[16] Zhou, S., et al., Comparative corrosion resistance of graphene sheets with different structures in waterborne epoxy coatings. Colloids and Surfaces A: Physicochemical and Engineering Aspects, 2018. 556: p. 273-283.

[17] Zhong, F., et al., Self-assembled graphene oxide-graphene hybrids for enhancing the corrosion resistance of waterborne epoxy coating. Applied Surface Science, 2019. 488: p. 801-812.

[18] Ye, Y., et al., POSS-tetraaniline modified graphene for active corrosion protection of epoxy-based organic coating. Chemical Engineering Journal, 2020. 383: p. 123160.

[19] Verma, C., et al., Epoxy resins as anticorrosive polymeric materials: A review. Reactive and Functional Polymers, 2020. 156: p. 104741.

[20] Tanaka, Y. and H. Kakiuchi, Study of epoxy compounds. Part VI. Curing reactions of epoxy resin and acid anhydride with amine, acid, alcohol, and phenol as catalysts. Journal of Polymer Science Part A: General Papers, 1964. 2(8): p. 3405-3430.

[21] Hameed, N., et al., Rapid cross-linking of epoxy thermosets induced by solvate ionic liquids. ACS Applied Polymer Materials, 2020. 2(7): p. 2651-2657.

[22] Fu, K., et al., Molecular dynamics simulation and experimental studies on the thermomechanical properties of epoxy resin with different anhydride curing agents. Polymers, 2019. 11(6): p. 975.

[23] Nik Md Noordin Kahar, N.N.F., et al., The versatility of polymeric materials as self-healing agents for various types of applications: A review. Polymers, 2021. 13(8): p. 1194.

[24] Hang, T.T.X., et al., Corrosion protection mechanisms of carbon steel by an epoxy resin containing indole-3 butyric acid modified clay. Progress in Organic Coatings, 2010. 69(4): p. 410-416.

[25] Xiang, Q. and F. Xiao, Applications of epoxy materials in pavement engineering. Construction and Building Materials, 2020. 235: p. 117529.

[26] Dagdag, O., et al., Cyclotriphosphazene based dendrimeric epoxy resin as an anti-corrosive material for copper in 3% NaCl: Experimental and computational demonstrations. Journal of Molecular Liquids, 2020. 308: p. 113020.

[27] Dagdag, O., et al., Application of hexa propylene glycol cyclotriphosphazene as corrosion inhibitor for copper in 3% NaCl solution. Der Phar. Chem, 2015. 7(4).

[28] Galai, M., et al., The effect of temperature on the inhibition of acid hydrochloric corrosion of carbon steel by hexa propylene glycol cyclotriphosphazene. Journal of Chemical and Pharmaceutical Research, 2015. 7(10): p. 712-719.

[29] Masood, S., et al., Fabrication of cardanol (a phenolic lipid) based polyamine coatings for anti-corrosive applications. Progress in Organic Coatings, 2023. 174: p. 107304.

[30] Khan, A.A., et al., Investigating the effect of curing temperature on the corrosion resistance of epoxy-based composite coatings for aluminium alloy 7075 in artificial seawater. RSC advances, 2023. 13(30): p. 21008-21020.

[31] Jiang, F., et al., Anti-corrosion behaviors of epoxy composite coatings enhanced via graphene oxide with different aspect ratios. Progress in Organic Coatings, 2019. 127: p. 70-79.

[32] Khan, A.A., et al., Corrosion protection of aluminum alloy 7075 using functionalized micro-silica based epoxy coatings. Materials Research Express, 2023. 10(4): p. 045301.

[33] Khan, A.A., et al., Insights into the corrosion mitigation efficacy of modified SiO2/GO-based epoxy composite coatings for aluminum alloy AA6061 in marine applications. Journal of Coatings Technology and Research, 2024: p. 1-20.

[34] Tamilselvam, K., et al., Corrosion behavior of new rare-earth free Cu-based metallic glasses in NaCl solution of different molarity. Journal of Materials Research and Technology, 2022. 16: p. 482-494.